THE JOURNAL OF BIOLOGICAL CHEMISTRY Vol. 278, No. 16, Issue of April 18, pp. 14185–14195, 2003
Printed in U.S.A.

Efficient Initiation of HIV-1 Reverse Transcription *in Vitro*

REQUIREMENT FOR RNA SEQUENCES DOWNSTREAM OF THE PRIMER BINDING SITE ABROGATED BY NUCLEOCAPSID PROTEIN-DEPENDENT PRIMER-TEMPLATE INTERACTIONS*

Received for publication, November 14, 2002, and in revised form, January 29, 2003
Published, JBC Papers in Press, January 30, 2003, DOI 10.1074/jbc.M211618200

Yasumasa Iwatani‡§, Abbey E. Rosen¶‖, Jianhui Guo‡, Karin Musier-Forsyth¶, and Judith G. Levin‡**

From the ‡Laboratory of Molecular Genetics, NICHD, National Institutes of Health, Bethesda, Maryland 20892 and the ¶Department of Chemistry, University of Minnesota, Minneapolis, Minnesota 55455

Synthesis of HIV-1 (−) strong-stop DNA is initiated following annealing of the 3′ 18 nucleotides (nt) of $tRNA_3^{Lys}$ to the primer binding site (PBS) near the 5′ terminus of viral RNA. Here, we have investigated whether sequences downstream of the PBS play a role in promoting efficient (−) strong-stop DNA synthesis. Our findings demonstrate a template requirement for at least 24 bases downstream of the PBS when $tRNA_3^{Lys}$ or an 18-nt RNA complementary to the PBS (R18), but not an 18-nt DNA primer, are used. Additional assays using 18-nt DNA-RNA chimeric primers, as well as melting studies and circular dichroism spectra of 18-nt primer: PBS duplexes, suggest that priming efficiency is correlated with duplex conformation and stability. Interestingly, in the presence of nucleocapsid protein (NC), the 24 downstream bases are dispensable for synthesis primed by $tRNA_3^{Lys}$ but not by R18. We present data supporting the conclusion that NC promotes extended interactions between the anticodon stem and variable loop of $tRNA_3^{Lys}$ and a sequence upstream of the A-rich loop in the template. Taken together, this study leads to new insights into the initiation of HIV-1 reverse transcription and the functional role of NC-facilitated tRNA-template interactions in this process.

Human immunodeficiency virus type 1 (HIV-1)[1] DNA synthesis is initiated by annealing of the 3′ 18 nucleotides (nt) of a cellular tRNA primer, $tRNA_3^{Lys}$, to the complementary 18-nt primer binding site (PBS) near the 5′ end of the viral RNA template. Minus-strand DNA synthesis proceeds until the 5′ end of the template is copied, generating the first product of reverse transcription, a 200-nt DNA termed (−) strong-stop DNA ((−) SSDNA).

Studies on HIV-1 initiation *in vitro* indicate that two modes of synthesis are involved in this process: (i) initiation, characterized by a distributive, slow extension of the primer and a high dissociation rate of reverse transcriptase (RT) from the primer-template complex; and (ii) elongation, which follows a transition between incorporation of the sixth and seventh nt and results in a dramatic increase in the processivity and rate of DNA synthesis (1–5). The inability of HIV-1 RT to initiate (−) SSDNA synthesis efficiently *in vitro* may be in part due to the nature of the three-dimensional structure of the initiation complex, which involves extensive intermolecular interactions between the $tRNA_3^{Lys}$ primer and the RNA template (see below) (6–11). In addition, the efficiency of (−) SSDNA synthesis appears to be sensitive to the helical conformation of the nucleic acid duplexes that are accommodated by RT; for example, when an 18-nt DNA primer complementary to the PBS (D18) is used, (−) SSDNA synthesis begins immediately in the elongation mode (1–3, 5).

Initially, the 18-nt duplex region of the tRNA-viral RNA complex adopts an A-form helical geometry, but after incorporation of dNTPs, the primer-template complex becomes a DNA-RNA hybrid and assumes an intermediate conformation in solution (12–14). X-ray crystallographic structures of RT bound to primer-template complexes (D18 or RNA polypurine tract (PPT) primer annealed to a complementary DNA template) reveal a bend in these complexes of about 40° (15–17). The bend occurs where α-helix H in the thumb subdomain of RT contacts the bound nucleic acid (15–17) and is typically associated with a transition from A- to B-form geometry (17). It has been suggested that this structural transition is correlated with the transition from the initiation to elongation mode (3, 11).

The HIV-1 nucleocapsid protein (NC), a small basic protein with two zinc-finger structures (18), also functions in the initiation process. NC is a nucleic acid chaperone and catalyzes conformational rearrangements that lead to the most thermodynamically stable structures (19–30). The NC domain in Gag promotes tRNA primer placement on the RNA genome (31, 32), although the NC protein itself also has this activity *in vitro* (32–37). The zinc fingers are not required for the tRNA annealing reaction, either *in vitro* (34–37) or *in vivo* (31). However, there is evidence suggesting that the zinc fingers are needed to help form a functional initiation complex that promotes efficient (−) SSDNA synthesis (38, 39).

The importance of *cis*-acting elements in viral RNA for efficient (−) SSDNA synthesis was first demonstrated in studies with Rous sarcoma virus indicating that extended interactions between the U5-IR stem upstream of the PBS and the TΨC loop of $tRNA^{Trp}$ enhance initiation of reverse transcription (40, 41). More recently, an additional U5-TΨC interaction has been described (42). A novel interaction between the 5′ terminus of

* This work was supported in part by National Institutes of Health Grant AI65056 (to K. M.-F.). The costs of publication of this article were defrayed in part by the payment of page charges. This article must therefore be hereby marked "*advertisement*" in accordance with 18 U.S.C. Section 1734 solely to indicate this fact.

§ Recipient of a postdoctoral fellowship from the Japan Society for the Promotion of Science.

‖ Supported by National Institutes of Health Predoctoral Training Grant T32-GM08700.

** To whom correspondence should be addressed: Laboratory of Molecular Genetics, NICHD, Bldg. 6B, Rm. 216, NIH, Bethesda, MD 20892-2780. Tel.: 301-496-1970; Fax: 301-496-0243; E-mail: jlevin@mail.nih.gov.

[1] The abbreviations used are: HIV-1, human immunodeficiency virus type 1; nt, nucleotide(s); PBS, primer binding site; (−) SSDNA, (−) strong-stop DNA; RT, reverse transcriptase; PPT, polypurine tract; NC, nucleocapsid protein; TBE, Tris-borate/EDTA; T_m, melting point temperature.

$tRNA_3^{Lys}$ and the feline immunodeficiency virus U5-IR loop has also been reported (43). In the case of HIV-1, chemical and enzymatic probing revealed complex interactions between U5 sequences upstream of the PBS and the anticodon loop, the 3′ portion of the anticodon stem, and part of the variable loop of $tRNA_3^{Lys}$ (9–11, 44–46). In particular, both *in vitro* and *in vivo* data pointed to an interaction between the anticodon loop of $tRNA_3^{Lys}$ and an A-rich loop in HIV-1 RNA, approximately ten bases upstream of the PBS (1, 4, 8–10, 44, 46–52). The extended interactions between the primer tRNA and template have been reported to be stabilized by post-transcriptional modification of $tRNA_3^{Lys}$ (9) and to contribute to efficient initiation of (−) SSDNA synthesis and transition from the initiation to elongation mode (1). Recently, it was suggested that an interaction between the 5′ portion of the TΨC loop of $tRNA_3^{Lys}$ and a conserved 8-nt sequence in U5, referred to as a primer activation signal, may facilitate initiation of (−) SSDNA synthesis (53, 54).

As yet, a possible role in initiation for *cis*-acting template sequences downstream of the PBS has not been completely clarified. Deletion of a 54-nt sequence immediately downstream of the PBS led to a loss in infectivity and a dramatic reduction in viral DNA synthesis (55). Further analysis of smaller deletions within the 54-nt region showed that certain mutations have a greater effect on infectivity (55, 56) and synthesis of (−) SSDNA *in vivo* (55) than others. *In vitro*, however, the mutant RNA templates have similar activities but are less efficient than wild-type RNA in directing tRNA primer extension (4, 56). In other *in vitro* work, it was reported that templates with mutations in downstream sequences that disrupt base pairing with the proposed primer activation signal, direct increased levels of (−) SSDNA synthesis, compared with a wild-type RNA template (53, 54).

In the present study, we have investigated the primer and template requirements for efficient synthesis of (−) SSDNA *in vitro*. We report that in the absence of NC, at least 24 bases immediately downstream of the PBS are required for efficient (−) SSDNA synthesis when RNA primers (native $tRNA_3^{Lys}$ or an 18-nt RNA complementary to the PBS (R18)), but not an all DNA (D18) primer, are used. These findings, as well as results of assays with chimeric DNA-RNA primers, are correlated with CD spectra and melting studies of 18-nt primer:PBS duplexes, underscoring the important role of helical conformation and thermal stability for priming activity. The results also suggest that the presence of the 24 additional downstream bases in viral RNA may allow the template to assume a more favorable conformation for annealing to the RNA primers. Interestingly, HIV-1 NC abrogates the requirement for these additional bases if (−) SSDNA synthesis is primed by $tRNA_3^{Lys}$ but not by R18. Mutational analysis supports the hypothesis that the nucleic acid chaperone activity of NC facilitates stable formation of extended interactions between the 3′ anticodon stem and variable loop of $tRNA_3^{Lys}$ and bases upstream of the A-rich loop in the RNA template and that these interactions modulate initiation of reverse transcription.

EXPERIMENTAL PROCEDURES

Materials—Ribo- and deoxyribonucleosides are indicated by upper and lowercase letters, respectively. D18 and R18 oligonucleotides (5′-gtccctgttcgggcgcca and 5′-GUCCCUGUUCGGGCGCCA, respectively) that are complementary to the HIV-1 PBS were purchased from Oligos Etc., Inc. (Wilsonville, OR). Three DNA-RNA chimeric oligonucleotide primers, R9D9, D9R9, and R17D1, were prepared by solid-phase synthesis on an Expedite 8909 RNA/DNA synthesizer using phosphoramidite monomers, and other chemicals purchased from Glen Research (Sterling, VA). The sequences were as follows: 5′-GUCCCUGUUcgggcgcca (R9D9); 5′-gtccctgttCGGGCGCCA (D9R9); and 5′-GUCCCUGUUCGGGCGCCa (R17D1). Purified $tRNA_3^{Lys}$ from human placenta was obtained from Bio S&T (Lachine, Quebec, Canada). PCR primers and an 18-nt oligonucleotide complementary to the 3′ end of $tRNA_3^{Lys}$ (5′-tggcgcccgaacagggac) were purchased from Lofstrand (Gaithersburg, MD). [γ-^{32}P]ATP (3000 Ci/mmol) and [α-^{32}P]dCTP (6000 Ci/mmol) were purchased from Amersham Biosciences. HIV-1 RT was obtained from Worthington Biochemical Corp. (Lakewood, NJ). Calf intestinal phosphatase and Vent DNA polymerase were obtained from New England Biolabs (Beverly, MA). Recombinant wild-type HIV-1 NC (55-amino acid form) was a generous gift from Dr. Robert Gorelick and was prepared as described previously (57).

Plasmid Construction—All plasmid sequences were derived from the HIV-1 pNL4-3 clone (58). Plasmid pRUG, which was designed to provide the DNA templates for *in vitro* synthesis of viral RNA templates, was constructed from the previously described pJD plasmid (59). The pNL4-3 fragment from the *Sac*I site (nt 491) in the repeat (R) region of the 5′ long terminal repeat to the *Pst*I site (nt 1419) in the capsid coding region was inserted into the *Sac*I and *Pst*I sites of the pJD plasmid. Three mutations were made in pRUG, which result in modification of U5 sequences in the RNA transcribed from the mutant templates: pRUG mut (143–149), which changes nt 143–149 to their complementary bases; pRUG AloopU, which substitutes four U residues for the four A residues (nt 169–172) in the A-rich loop; and pRUG AloopU mut (143–149), containing the double mutation. For PCR amplification of fragments from plasmid pRUG, the forward primer (5′-ccaatgcttaatcagtgaggc), located at the start of the *amp* gene, 1459 nt upstream of the T7 promoter, was used. The reverse primers were as follows: pRUG mut (143–149), 5′-gtccctgttcgggcgccactgctagagattttccacactgactaaaagggtgactcccatctctagttacc; pRUG AloopU, 5′-gtccctgttcgggcgccactgctagagaaaaaccacactgactaaaagggtctgagggatctctagttacc; pRUG AloopU mut (143–149), 5′-gtccctgttcgggcgccactgctagagaaaaaccacactgactaaaagggtgactcccatctctagttacc. Each reverse primer has a *Nar*I site starting 11 nt from the 5′ end (corresponding to nt 184–190 in the PBS region of the RNA); the vector also has a *Nar*I site. The fragments were cut with *Nar*I and inserted into *Nar*I-digested pRUG. In all cases, the sequences of both the insert and the boundary regions were verified by DNA sequencing.

Preparation of RNA Templates—To make the DNA templates for *in vitro* RNA transcription, the fragments containing both the T7 promoter and the desired length of viral RNA were amplified by PCR from plasmid pRUG or the three pRUG mutants, using Vent DNA polymerase. The forward primer (5′-ccaatgcttaatcagtgaggc) is located at the start of the *amp* gene. The reverse primers were as follows: RNA 200, 5′-gtccctgttcgggcgccact; RNA 210, 5′-tcgctttcaagtccctgttc; RNA 220, 5′-ggctttactttcgctttcaa; RNA 221, 5′-tggctttactttcgctttca; RNA 222, 5′-ctggctttactttcgctttc; RNA 223, 5′-tctggctttactttcgcttt; RNA 224, 5′-ctctggctttactttcgctt; RNA 226, 5′-tcctctggctttactttcgc; RNA 228, 5′-tctcctctggctttactttc; RNA 230, 5′-gatctcctctggctttactt; RNA 240, 5′-tgcgtcgagagatctcctct; RNA 244, 5′-gtcctgcgtcgagagatc; RNA 732, 5′-gtaattttggctgacctggc. The reverse primers for RNA 200 and RNA 244 could also be used to generate the corresponding mutant RNA templates. After PCR amplification, the DNA fragments were separated on 1.5% agarose gels and were extracted with a QIAEX II kit (Qiagen, Inc., Valencia, CA). To prepare the DNA template for synthesis of RNA 509, pRUG was linearized with *Acc*I. RNA templates were transcribed with T7 RNA polymerase, using an Ambion MEGAscript kit (Ambion Inc., Austin, TX) and were then purified by electrophoresis on a 2 or 3% agarose gel. RNA fragments of the appropriate size were extracted from the gel with an RNaid kit (Qbiogene, Carlsbad, CA), according to the manufacturer's instructions. The purified RNA was quantified by measuring the absorbance at 260 nm. Note that the RNA templates are defined by the number of bases downstream of nt +1 in the viral RNA genome (see Fig. 1*B*). The secondary structure of a portion of the 5′ leader region of HIV-1 NL4-3 RNA (see Fig. 1*A*) was predicted from *mfold* (60, 61).

Preparation of Labeled Primers—The R18, R9D9, D9R9, and R17D1 primers were purified on denaturing 20% polyacrylamide-Tris-borate/EDTA (TBE) gels and were then eluted with an RNaid kit. All of the 18-nt primers were labeled at their 5′ ends with [γ-^{32}P]ATP, as described previously (62). To prepare 5′ ^{32}P-labeled $tRNA_3^{Lys}$, the acceptor stem was first disrupted by annealing the 3′ end of the tRNA to an 18-nt DNA complementary oligonucleotide (see above); this increases the efficiency of labeling at the 5′ end of the tRNA. The tRNA was then dephosphorylated with calf intestinal phosphatase (1 unit/μg of $tRNA_3^{Lys}$) at 50 °C for 2 h prior to labeling. Following incubation with 0.2 units/μl of RNase-free DNase I (Ambion Inc.) for 30 min at 37 °C, the 76-nt tRNA was separated from other products by electrophoresis on a denaturing 10% polyacrylamide-TBE gel and was then eluted and quantified, as described above under "Preparation of RNA Templates."

Assay of (−) SSDNA Synthesis—Unless specified otherwise, the template and primer were annealed with heat, and NC was not present in

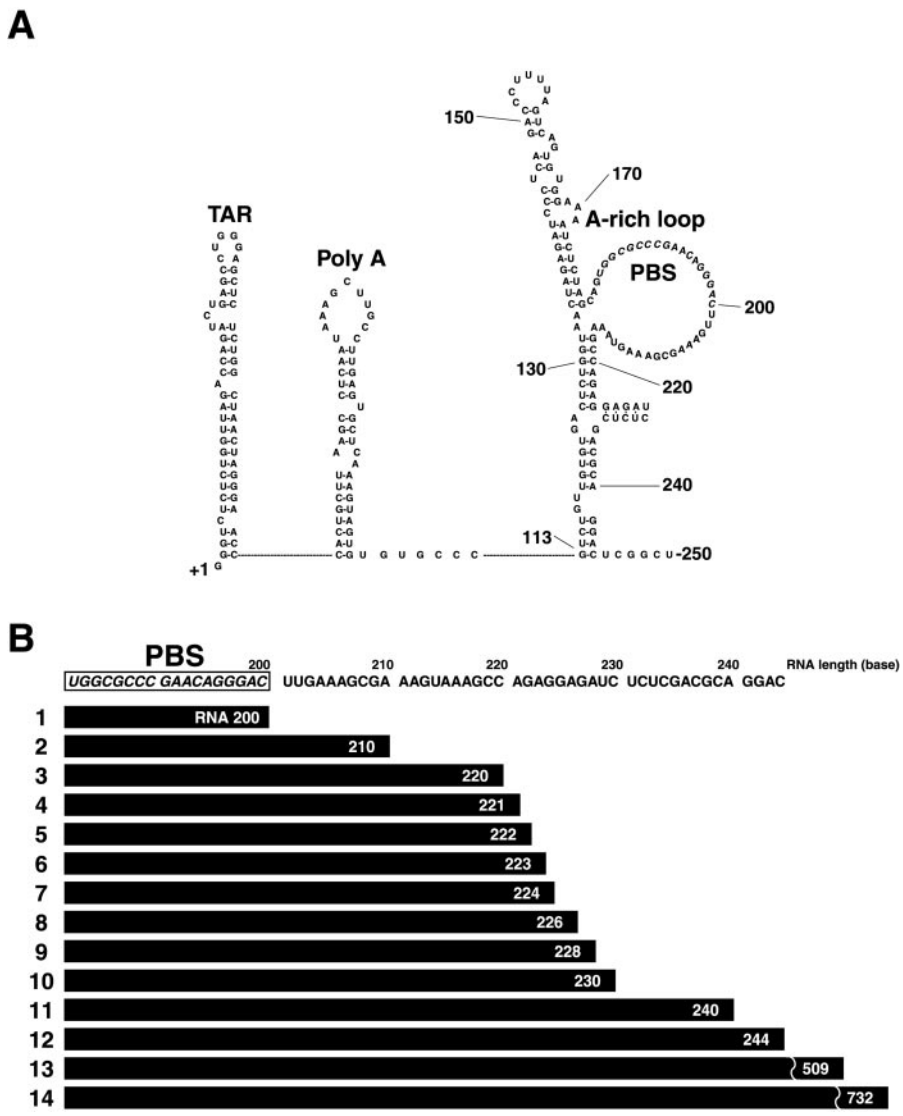

FIG. 1. **Proposed secondary structure of a portion of the HIV-1 NL4-3 5′ leader region and schematic diagram of RNA templates used in this study.** *A*, the predicted secondary structure of a portion of the 5′ leader region of HIV-1 NL4-3 RNA obtained using *mfold* (60, 61). The TAR stem-loop, the poly(A) hairpin, the A-rich loop, and the 18-nt PBS are indicated. The PBS bases are shown in *italics*. Note that throughout the text, upstream sequences refers to template RNA sequences 5′ of the PBS, *i.e.* beginning at nt 182; downstream sequences refers to template sequences 3′ of the PBS, *i.e.* beginning at nt 201. *B*, the *boxed* PBS sequence (nt 183–200) and the sequence of downstream bases up to nt 244 are shown at the *top* of the *panel*. The templates start from an additional G residue upstream of nt +1 in viral genomic RNA and are designated according to their total number of bases.

the reaction mixture. In these experiments, 0.2 pmol of the indicated RNA template was annealed to 0.1 pmol of the indicated ^{32}P-labeled primer (3–5 × 10^5 cpm) in 2 μl of buffer, containing 50 mM Tris-HCl, pH 8.0, and 75 mM KCl at 65 °C for 5 min followed by gradual cooling to 37 °C. Where annealing was performed in the presence of HIV-1 NC, 0.2 pmol of the RNA template was annealed to 0.1 pmol of the 5′ labeled R18 primer (3–5 × 10^5 cpm) or to unlabeled $tRNA_3^{Lys}$ in 7 μl of solution, containing 50 mM Tris-HCl, pH 8.0, 75 mM KCl, and NC protein (equivalent to 7 nt per NC) at 37 °C for 15 min. Following annealing, reaction buffer (50 mM Tris, pH 8.0, 75 mM KCl, 7 mM $MgCl_2$, 1 mM dithiothreitol, 50 μM dNTPs) and HIV-1 RT (0.2 pmol) were added, and the mixture (final volume, 20 μl) was incubated at 37 °C for 30 min. When unlabeled $tRNA_3^{Lys}$ was used, the reaction buffer also contained 10 μCi of [α-^{32}P]dCTP. Reactions were terminated by freezing on dry ice, followed by addition of 8 μl of gel loading buffer II (Ambion). The samples were heated at 90 °C for 5 min and were loaded onto a denaturing 6% polyacrylamide-TBE gel. Radioactivity was quantified by using a PhosphorImager (Molecular Dynamics) and ImageQuant software. To calculate the percentage of the (−) SSDNA product that was extended from a 5′ labeled primer, the "volume" of the (−) SSDNA band was divided by the total volume in that lane. For experiments where (−) SSDNA was internally labeled, the amount of (−) SSDNA product made with a particular RNA template relative to RNA 200 (taken as 100%) was calculated. Each experiment was repeated independently at least three times. Representative data are shown under "Results."

CD Spectra—For CD spectra, R18, D18, and chimeric DNA-RNA oligonucleotides were gel-purified on denaturing 16% polyacrylamide-TBE gels, eluted, and desalted as described (63, 64). To determine the concentration of the synthetic oligonucleotides, an extinction coefficient (ϵ_{260}) of 14.3 × 10^5 $M^{-1}cm^{-1}$ was used. CD spectra were obtained on a Jasco J-710 spectropolarimeter at 25 °C in a 1-mm cell with ~25 μM duplex. The duplexes were annealed by incubating strands in buffer containing 50 mM Tris-HCl, pH 8.0, and 75 mM KCl at 80 °C for 2 min, 60 °C for 2 min, followed by addition of 0.1 M $MgCl_2$ to a final concentration of 10 mM and placement on ice. Final CD spectra are the average of three scans.

Melting Studies—UV melting profiles (absorbance *versus* temperature) were obtained on an Agilent 8453 spectrophotometer equipped with a Peltier device. Samples were heated at 15 degrees/h, and the absorbance at 260 nm was collected at 0.5-degree increments from 40 to 98 °C in a 1-cm path length cuvette. Prior to data collection, duplexes (2 μM) were annealed in 50 mM Tris-HCl, pH 8.0, and 75 mM KCl by incubating at 65 °C for 5 min, slow cooling to 37 °C, incubating at 37 °C for 5 min, and then placing on ice. Reported melting point temperature (T_m) values were calculated using the first derivative of the heating trace and represent the average of two or three trials, which differed by <3.2%.

RESULTS

Effect of RNA Template Length on (−) SSDNA Synthesis Primed by the D18, R18, and $tRNA_3^{Lys}$ Primers—To investigate the potential role of sequences downstream of the PBS in the synthesis of (−) SSDNA (Fig. 1*A*), we analyzed primer extension efficiency with 14 *in vitro* transcribed RNA templates containing varying lengths of downstream sequences (Fig. 1*B*). The templates tested in the initial experiments terminated at nt 200 *i.e.* the 3′ end of the PBS (RNA 200), nt 244 (RNA 244), nt 509 (RNA 509), and nt 732 (RNA 732). The results showed

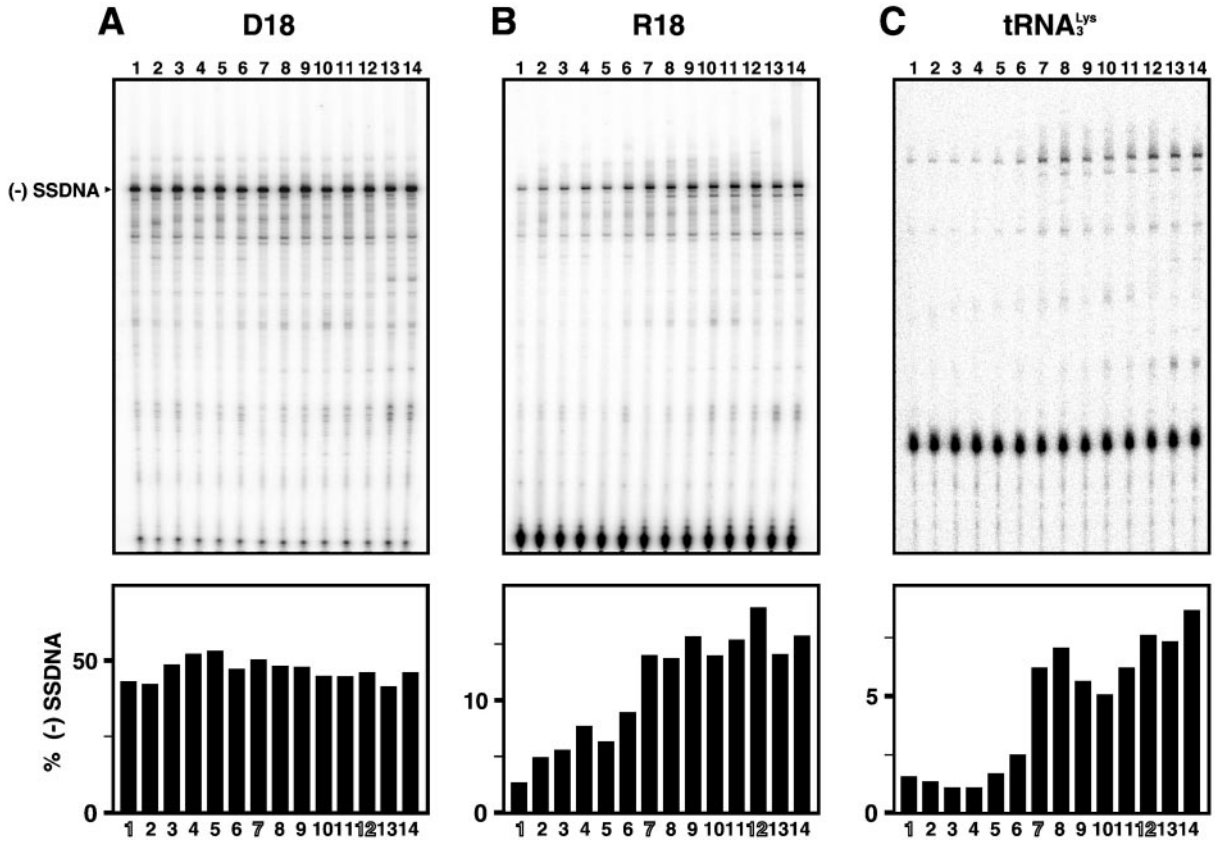

FIG. 2. **(−) SSDNA synthesis initiated by D18, R18, and $tRNA_3^{Lys}$ primers.** D18 (*A*), R18 (*B*), and $tRNA_3^{Lys}$ (*C*) primers were used to initiate (−) SSDNA synthesis, as described under "Experimental Procedures." The *upper portions* of each *panel* show gel analysis of the ^{32}P-labeled products; the position to which (−) SSDNA migrated is also indicated. PhosphorImager analysis of the gel data is shown in the *bar graphs* in the *lower portion* of each *panel*; the percentage (%) of (−) SSDNA was calculated as described under "Experimental Procedures." *Lane 1*, RNA 200; *lane 2*, RNA 210; *lane 3*, RNA 220; *lane 4*, RNA 221; *lane 5*, RNA 222; *lane 6*, RNA 223; *lane 7*, RNA 224; *lane 8*, RNA 226; *lane 9*, RNA 228; *lane 10*, RNA 230; *lane 11*, RNA 240; *lane 12*, RNA 244; *lane 13*, RNA 509; *lane 14*, RNA 732. The *numbers* corresponding to *lanes 1* (RNA 200), *7* (RNA 224), and *12* (RNA 244) are *highlighted*.

that at most, 44 downstream bases were required for efficient priming with the R18 primer consisting of the 3′ 18 nt of $tRNA_3^{Lys}$ or with full-length native $tRNA_3^{Lys}$ (data not shown).

To more closely determine the minimum number of downstream bases required for efficient synthesis of (−) SSDNA, additional templates with smaller differences in template length were tested. A summary of our observations is presented in Fig. 2, which shows (−) SSDNA synthesis initiated with the D18 (Fig. 2*A*), R18 (Fig. 2*B*), and $tRNA_3^{Lys}$ (Fig. 2*C*) primers, using the 14 viral RNA templates (Fig. 1*B*). DNA products were separated by polyacrylamide gel electrophoresis (*upper portion* of each *panel*), and the percent (−) SSDNA synthesized was calculated from PhosphorImager analysis of the gel data (*lower portion* of each *panel*).

As demonstrated in Fig. 2*A*, (−) SSDNA synthesis primed by the D18 primer was independent of template length. However, with the R18 or $tRNA_3^{Lys}$ primers and templates RNA 200 to RNA 223, each consecutive addition of downstream bases resulted in corresponding increases in the amount of (−) SSDNA synthesis (Fig. 2, *B* and *C*, *lanes 1–6*). However, once the template contained 24 downstream bases, adding more bases to the template did not lead to a further increase in (−) SSDNA synthesis (Fig. 2, *B* and *C*, *lanes 7–14*). These results indicate that the RNA template must contain 24 bases downstream of the PBS for efficient RT-catalyzed extension *in vitro*.

To investigate whether efficient RT extension requires a specific sequence in the RNA genome or whether a random sequence of 24 bases downstream of the PBS is sufficient, two different RNA templates (RNA 224a and RNA 224b) were prepared. RNA 224a was constructed by removing the 44 bases immediately downstream of the PBS but retaining the next 3′ 24 bases; similarly, in RNA 224b, the 24 bases immediately downstream of the PBS were deleted, but the succeeding 3′ 24 bases were retained. Using these two RNA templates and the R18 primer, (−) SSDNA synthesis was even lower than that observed with RNA 200 (data not shown). Thus, the effect of the 24-base sequence downstream of the PBS on efficient primer extension is dependent on the specific genomic RNA sequence, presumably because it allows the RNA template to fold into a stable conformation that is favorable for duplex formation.

(−) SSDNA Synthesis Primed by DNA-RNA Chimeric Primers—To gain further insight into the unique dependence of RNA primers on template length, we compared the activities of chimeric primers that were complementary to the PBS: R9D9 (Fig. 3*A*), D9R9 (Fig. 3*B*), and R17D1 (Fig. 3*C*). The experimental procedures were the same as those used for the experiments described in the previous section. As shown in Fig. 3*A*, the percent (−) SSDNA synthesis primed by the R9D9 primer (5′ half RNA, 3′ half DNA) was similar with all 14 RNA templates. This result indicates that R9D9 behaves like the all-DNA primer, D18 (compare Fig. 2*A* and Fig. 3*A*).

In contrast, when synthesis was primed by R17D1 (substitution of only one deoxyribonucleotide at the 3′ end of R18), the efficiency of (−) SSDNA synthesis was dependent on the length of the downstream sequences (Fig. 3*C*). Thus, RNA templates that had 24 or more downstream bases (Fig. 3*C*, *lanes 7–14*) supported similar levels of (−) SSDNA synthesis, whereas with

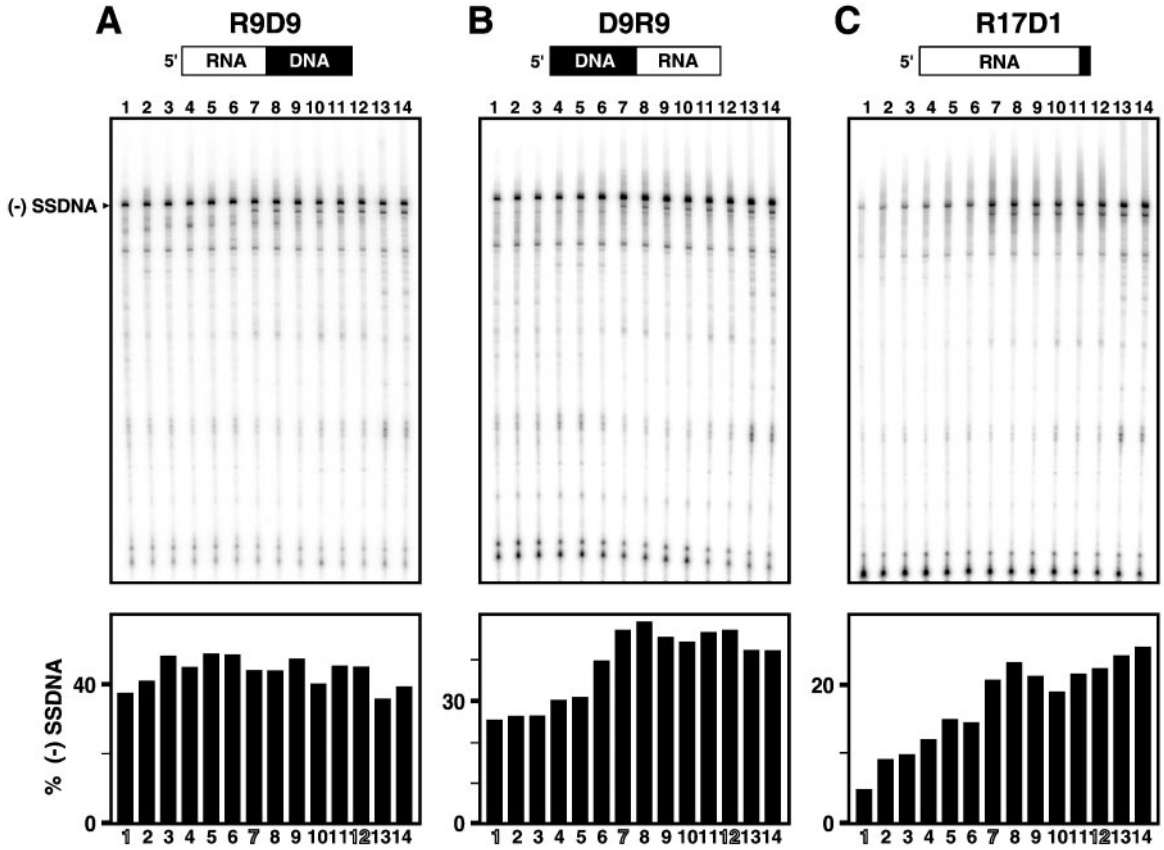

FIG. 3. **(−) SSDNA synthesis initiated by DNA-RNA chimeric primers.** Three DNA-RNA chimeric primers, R9D9 (*A*), D9R9 (*B*), and R17D1 (*C*), were used to initiate (−) SSDNA synthesis, as described under "Experimental Procedures." The RNA and DNA portions of each primer are represented at the *top* of each *panel* by *white* and *black boxes*, respectively. The gel data are shown in the *upper portion* of each *panel*. PhosphorImager analysis of the gel data (*lower portion* of each *panel*) and calculation of the (%) (−) SSDNA product were performed as described in the legend to Fig. 2. The identities of the RNA templates in *lanes 1–14* are the same as in Fig. 2.

templates having a total of 200–223 bases (RNA 200 to RNA 223), incremental increases in the length of the template led to corresponding increases in (−) SSDNA (Fig. 3*C*, *lanes 1–6*). These findings demonstrate that R17D1 behaves like the all-RNA primer, R18 (compare Fig. 3*C* with Fig. 2*B*). Interestingly, when the D9R9 primer (5′ half DNA, 3′ half RNA) was used, maximal (−) SSDNA synthesis was achieved only if the template contained at least 24 bases downstream of the PBS (Fig. 3*B*). However, the dependence on template length was not as striking as that seen with the R17D1 and R18 primers (compare Fig. 3*B* with Fig. 3*C* and Fig. 2*B*, respectively). Taken together, the observations illustrated in Fig. 3 raise the possibility that differences between the helical conformations of duplexes formed by the PBS and each of the oligonucleotide primers might be responsible for the observed differences in the requirements for priming activity.

CD Spectra of Duplexes between the PBS (Template) and Various Oligonucleotide Primers—To investigate the possibility that helical conformation may be a determinant for priming activity, we analyzed the CD spectra of 18-nt primer:PBS duplexes (Fig. 4). The CD spectra of the all-RNA duplex (R18:PBS), as well as the various deoxy-substituted chimeric duplexes, indicated overall A-form helices for all variants tested. All spectra had a large maximum near 265 nm, a shallow negative peak close to 235 nm, and a large negative peak around 210 nm. A very small negative peak was also observed near 300 nm in all cases. Although the duplexes all appeared to maintain an overall A-form geometry, which is in good agreement with earlier CD studies of DNA:RNA hybrids (65–68), slight shifts in the spectra were apparent in some cases, suggesting subtle differences in the conformations.

Replacement of R18 with D18 resulted in noticeable alteration of the CD spectrum (Fig. 4). Both a decrease and a slight shift in the maximum of the D18:PBS spectrum compared with that of R18:PBS suggested that the hybrid duplex, although maintaining an overall A-form conformation, had characteristics that are shifted somewhat toward B-form (69). In particular, the negative CD band around 298 nm present in the RNA duplex was more shallow and shifted to ~308 nm in the D18:PBS spectrum (Fig. 4, *insets*), which is indicative of a shift toward B-form conformation (69). Thus, the CD spectrum observed with the D18:PBS duplex suggests that the lack of dependence on template length in the extension assays (Fig. 2*A*) with a DNA primer may be the result of an altered duplex conformation.

Spectra for R9D9:PBS and D9R9:PBS indicated that the conformations of these chimeric duplexes were also slightly altered relative to those of R18:PBS and D18:PBS. The R9D9:PBS CD spectrum (Fig. 4*A*) had a maximum near 265 nm and a shallow negative band near 300 nm (Fig. 4*A*, *inset*) that both shifted slightly toward longer wavelengths relative to the R18:PBS duplex. Overall, the spectrum aligns more closely with that of D18:PBS than with the spectrum of the all-RNA duplex and indicates a slight shift toward a B-form conformation. This conformational change toward B-form is again correlated with a lack of dependence on downstream template sequences in the reverse transcription assays carried out with the R9D9 primer (Fig. 3*A*). In contrast, the CD spectrum of D9R9:PBS was more similar to that of the all-RNA (R18:PBS) duplex (Fig. 4*B*). The most significant change in the D9R9:PBS spectrum was a decrease in the strength of the maximum at 265 nm. This may indicate a minor shift toward B-form and/or a decrease in

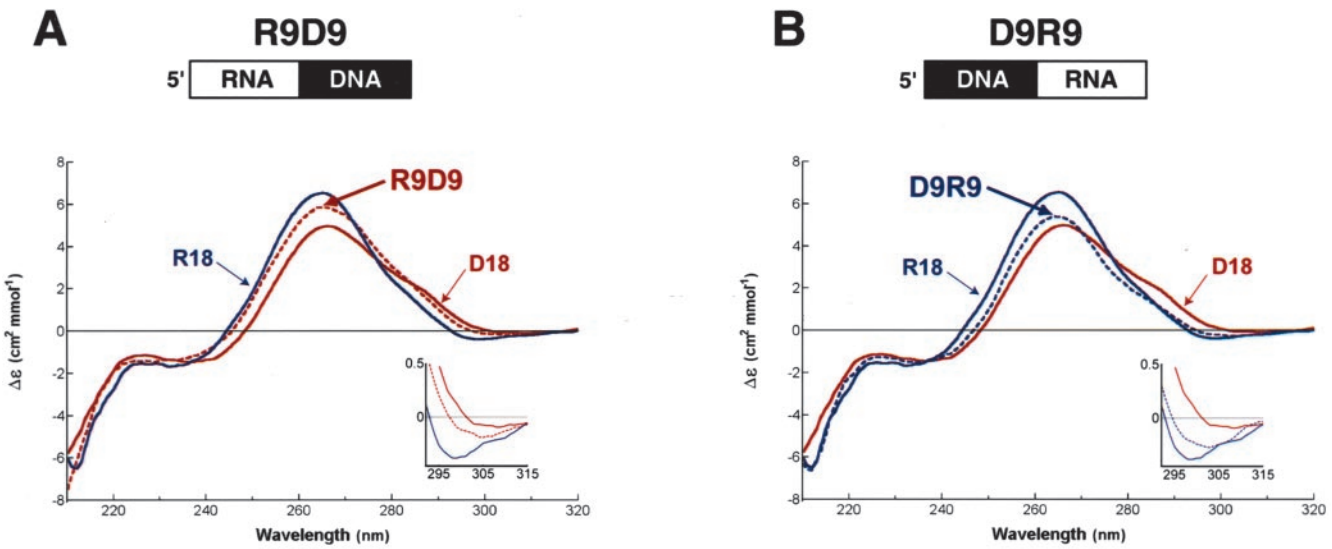

FIG. 4. **CD spectra of 18-nt primer:PBS duplexes.** The figure represents CD spectra of primer:PBS duplexes (25 μM) in 50 mM Tris-HCl, pH 8.0, 75 mM KCl, and 10 mM $MgCl_2$ at 25°C. Comparison of CD spectra of R9D9:PBS (*dashed red*) (*A*) and D9R9:PBS (*dashed blue*) (*B*) with those of R18:PBS (*solid blue*) and D18:PBS (*solid red*) is shown. *Insets*, wavelength region 295–315 nm illustrates the shift in shallow negative CD bands.

overall stability. The minor deviations from the all-RNA duplex observed in the CD spectrum of the D9R9:PBS duplex are in accord with the slight deviation in behavior of the D9R9 primer relative to the all-RNA, R18 primer in the reverse transcription assays (Fig. 3*B*).

By overlaying the spectra of the R17D1:PBS and R18:PBS duplexes, it is evident that they are essentially identical (data not shown). Therefore, there is no change in the duplex conformation when a single deoxyribonucleotide is substituted at the 3′ end of the primer strand. The similarity in conformation is in accord with the similar dependence on downstream sequences in the initiation of reverse transcription when R17D1 is substituted for R18 (Fig. 3*C*).

Thus, CD analysis suggests that there is a correlation between the helical conformation of the various primer:PBS duplexes and their priming activity. In particular, we find that an increased dependence on template length in the assays that measure the ability of the primers to initiate (−) SSDNA synthesis correlates with A-form helical geometry (compare Fig. 4 with Figs. 2 and 3). In contrast, the duplexes that exhibit a shift toward B-form geometry display priming activity that is relatively independent of downstream sequences.

Melting Studies of Duplexes between the PBS (Template) and Various Oligonucleotide Primers—Melting studies were undertaken to investigate the thermal stability of the primer-template duplexes (Table I). As expected, the all-RNA duplex was more stable than the all-DNA duplex (66, 70, 71), whereas the chimeras were intermediate in their thermal stability. The relative stability of chimeric DNA-RNA duplexes is difficult to predict and depends strongly on base composition (65–67, 70, 71). Interestingly, we find that the R9D9:PBS duplex had a T_m of 78.5 °C, which is very close to the T_m for the D18 duplex (77.5 °C); in contrast, the D9R9 duplex had a T_m (84.5 °C) that is more similar to the T_m for the R18 duplex (88.1 °C). These data indicate that the R9D9 duplex is more DNA-like in its stability, whereas the D9R9 duplex is more RNA-like. Thus, the results are in excellent agreement with the biochemical data (see Figs. 2 and 3) and CD analysis (Fig. 4) described above.

Effect of NC on the Requirement for Downstream Bases in Reactions Primed by R18 or $tRNA_3^{Lys}$—HIV-1 NC activity appears to be necessary to form a functional initiation complex (38, 39) and achieve efficient synthesis of (−) SSDNA. It was

TABLE I
Melting temperatures of primer:PBS duplexes

All measurements were carried out in 50 mM Tris-HCl, pH 8.0, and 75 mM KCl and represent the average of two or three trials, which differed by <3.2%.

Primer	T_m (°C)
D18	77.5
R9D9	78.5
D9R9	84.5
R18	88.1

therefore of interest to investigate the requirement for downstream bases in reactions containing NC. In Fig. 5*A*, R18 (labeled at its 5′ end) was annealed to the RNA templates in the presence of NC (7 nt/NC), and this was followed by RT-catalyzed extension of the primer to yield (−) SSDNA. The results showed that the percent (−) SSDNA was independent of template length only when ≥24 bases downstream of the PBS were included in the template (Fig. 5*A*, compare *lanes 7–12* with *lanes 1–6*). This result is identical to that observed when NC was absent from the reaction and the primer:template duplex was formed by heat annealing (Fig. 2*B*).

To perform the analogous experiment with native $tRNA_3^{Lys}$, unlabeled primer was annealed to the RNA templates in the presence of NC, and DNA products were internally labeled by adding [α-^{32}P]dCTP to the reaction mixtures (Fig. 5*B*). Interestingly, in this case, approximately the same amount of (−) SSDNA was synthesized with each of the templates. This finding is illustrated by the *bar graph* in the *lower portion* of Fig. 5*B*, where the amount of (−) SSDNA synthesized with each template was plotted relative to the amount made by RNA 200.

The results of Fig. 5 demonstrate that NC was able to abrogate the requirement for downstream bases seen with templates RNA 200 to RNA 223 when $tRNA_3^{Lys}$ (Fig. 5*B*), but not when the R18 primer (Fig. 5*A*), was used. Similar results were obtained when unmodified (synthetic) $tRNA_3^{Lys}$ was added to RNA 200 reactions, *i.e.* without NC, (−) SSDNA synthesis was dependent on sequences downstream of the PBS, but in the presence of NC it was not. However, in these reactions, the level of (−) SSDNA synthesis was reduced by ~2–3-fold relative to the amount made in comparable reactions with the native tRNA primer (data not shown). It should also be noted

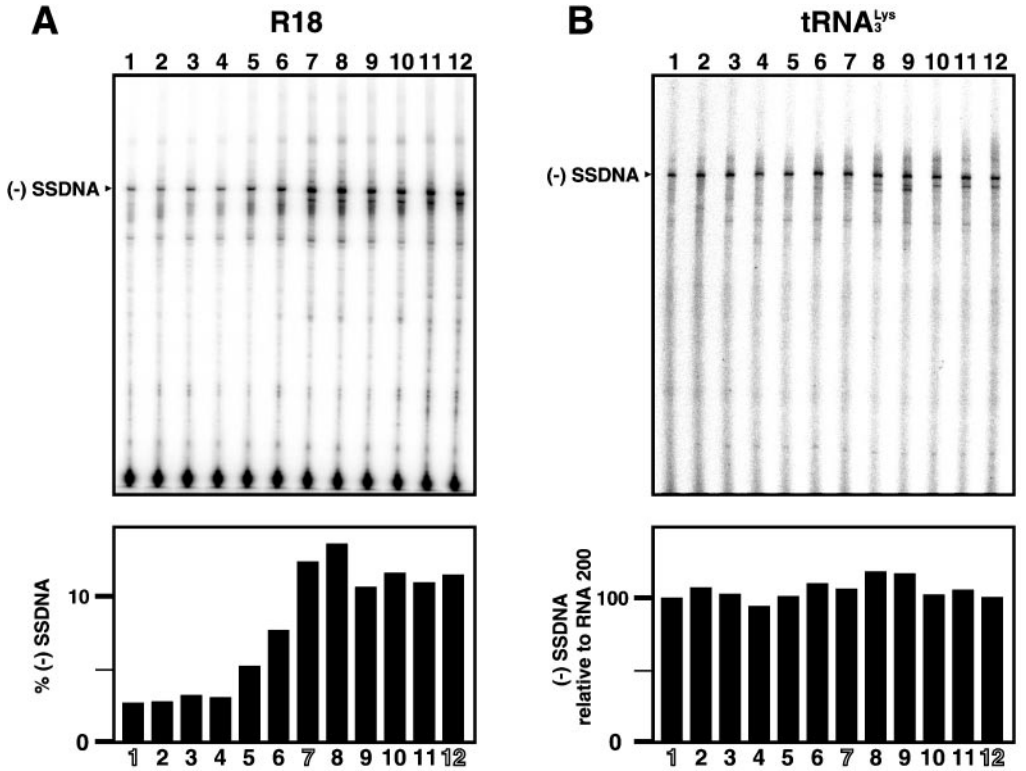

FIG. 5. **Effect of NC on (−) SSDNA synthesis initiated by the R18 and $tRNA_3^{Lys}$ primers.** 5′ ^{32}P-labeled R18 (*A*) or unlabeled native $tRNA_3^{Lys}$ (*B*) were annealed to RNA templates in the presence of NC and were extended by HIV-1 RT, as detailed under "Experimental Procedures." Gel data are shown at the *top* of each *panel*. PhosphorImager analysis of the gel data (*lower portion* of each *panel*) and calculation of percent (−) SSDNA (*A*) or (−) SSDNA relative to RNA 200 (*B*) were performed as described under "Experimental Procedures." The identities of the RNA templates in *lanes 1–12* are the same as in Fig. 2.

that addition of NC following heat annealing gave the same results as those obtained when NC was maintained in the mixture during annealing and extension (data not shown), in agreement with Brulé *et al.* (72). Thus, using either protocol with the native tRNA primer, the 24-nt downstream element was dispensable for efficient (−) SSDNA synthesis.

Effect of Mutating Template Bases Upstream of the PBS on the Ability of NC to Abrogate the Requirement for the Downstream Element—The results illustrated in Fig. 5, demonstrating a specific effect of NC with the tRNA primer, but not with R18, suggest that NC may facilitate extended interactions between $tRNA_3^{Lys}$ and upstream template sequences and that these interactions modulate reverse transcription. Previous work (1, 4, 8–10, 44, 46–52) indicated that residues in the A-rich loop interact with the anticodon loop of the tRNA primer. In addition, structure probing suggested an interaction between the 3′ arm of the anticodon stem and the variable loop of the tRNA (nt 40–46) and U5 sequences upstream of the A-rich loop, corresponding to nt 140–143 in helix 3E and nt 158–160 in helix 5D in HIV-1 MAL RNA (10, 44, 46). In HIV-1 NL4-3, used in the present work, we find that the corresponding template sequences are contiguous and include nt 143–149 (58).

To investigate whether such extended tRNA-template interactions could account for the NC effect on $tRNA_3^{Lys}$-primed synthesis of (−) SSDNA, two different substitution mutations (Fig. 6) were made in both the RNA 200 and RNA 244 templates, either singly or in combination: (i) mutation of the four A residues at nt 169–172 to U residues (AloopU); (ii) mutation of nt 143–149 (mut (143–149)) to the complementary bases; and (iii) the double mutation. Each of the templates was assayed with unlabeled $tRNA_3^{Lys}$ primer, in the absence or presence of NC. A representative gel and PhosphorImager analysis of gel data averaged from three independent experiments are shown in Fig. 7, *A* and *B*, respectively. In Fig. 7*B*, the results are expressed as the amount of (−) SSDNA made relative to that synthesized by the wild-type RNA 244 template in the absence of NC (100%).

As expected from the data of Fig. 5, reactions with the wild-type RNA 244 template yielded the same amount of (−) SSDNA independent of the presence of NC, whereas with the RNA 200 template, the amount of synthesis reached the RNA 244 level only when NC was added (Fig. 7, *A* and *B*, compare *lanes 5* and *13* with *lanes 1* and *9*). The RNA 200 and RNA 244 templates bearing the AloopU mutation exhibited an increase in priming efficiency (ranging from ~1.5- to 3-fold) in the presence of NC (Fig. 7, *A* and *B*, *lanes 10* and *14*), compared with the RNA 244 control (Fig. 7, *A* and *B*, *lane 5*); with the RNA 244 mutant, a similar effect was also seen in the absence of NC (Fig. 7, *A* and *B*, *lane 6*). Under conditions where the initial products of reverse transcription (+1, +3, and +5 nt) can be easily detected (low dNTP concentrations), overall accumulation of these short DNAs in NC-containing mutant reactions was significantly reduced, relative to the wild-type controls. However, unlike the corresponding wild-type templates, the AloopU mutants directed synthesis of a greater amount of the +5 product relative to the +1 and +3 products (data not shown). These results are in agreement with findings by Liang *et al.* (4) that disrupting the interaction between the A-rich loop in the template and the anticodon loop of the tRNA primer leads to a decrease in RT pausing *in vitro*.

In contrast to our observations with the AloopU mutants, mutation of nt 143–149 alone or in combination with the AloopU mutation reduced the activity of RNA 200 by about 2-fold in the absence of NC (Fig. 7, *A* and *B*, *lanes 3* and *4*). With the RNA 244 template, these mutations supported a modest to very slight increase in (−) SSDNA synthesis (Fig. 7, *A* and *B*, *lanes 7* and *8*, respectively). Most importantly, however, in the

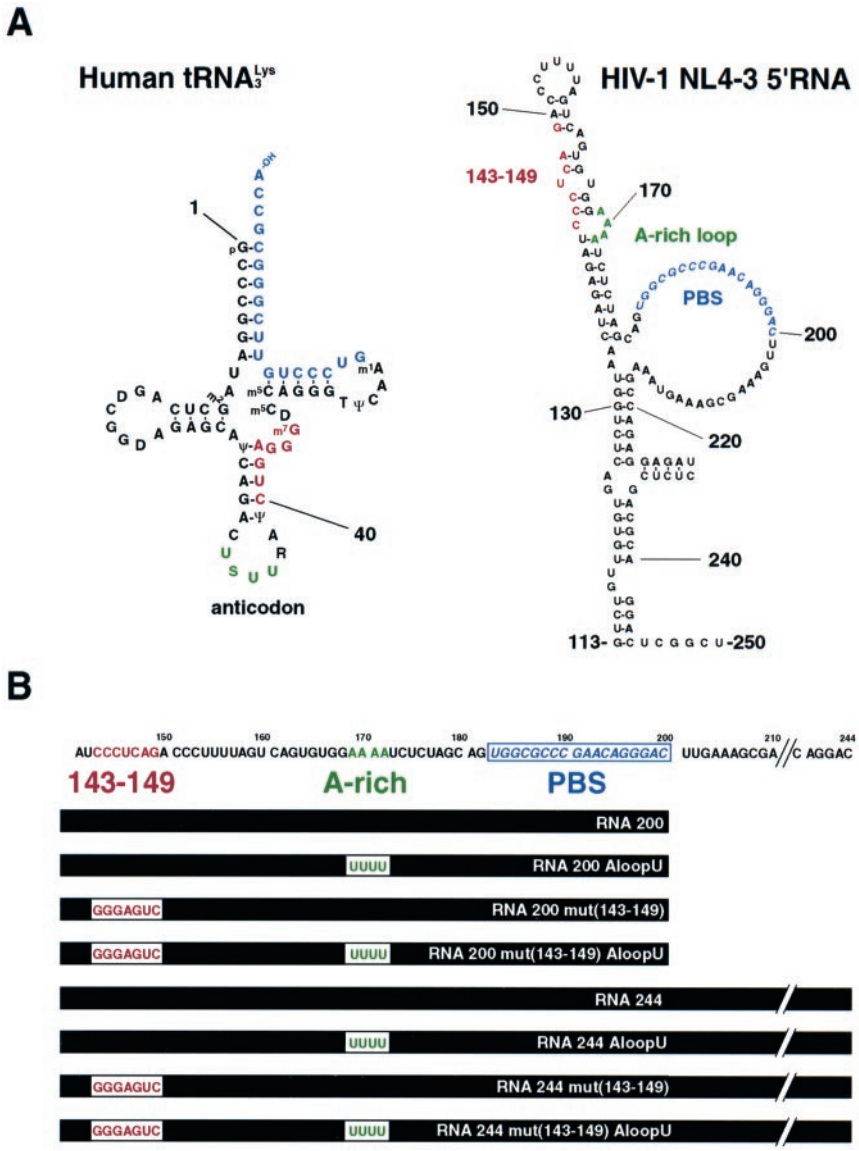

FIG. 6. **Mutations in RNA template bases upstream of the PBS.** *A*, the entire sequence of the 76-nt human $tRNA_3^{Lys}$ and sequences from nt 113–250 at the 5′ end of NL4-3 genomic RNA are shown. The PBS (*italics*) and the 3′ acceptor stem in the tRNA are in *blue*. Upstream RNA sequences nt 143–149 and the complementary sequence in the 3′ arm of the anticodon stem and variable loop of $tRNA_3^{Lys}$ (nt 40–46) are in *red*; the A-rich loop (nt 169–172) and the complementary anticodon loop in the tRNA are in *green*. *B*, the linear template sequence is shown with the three regions, nt 143–149, A-rich loop, and PBS, *highlighted* with the same colors as those used in *A*. A schematic representation of the wild-type and mutant RNA 200 and RNA 244 templates indicating the mutated sequences is shown *below* the *linear sequence*.

presence of NC, there was a major difference in the activities of the mutant RNA 200 and RNA 244 templates. Thus, when the RNA 200 template contained either the 143–149 mutation or the double mutation, there was an ~16-fold decrease in activity (Fig. 7, *A* and *B*, *lanes 11* and *12*). Interestingly, the actual amount of (−) SSDNA made with these two mutants was the same with or without NC (compare *lanes 3* and *4* with *lanes 11* and *12*). However, RNA 244 mut (143–149) and the double mutant had the same or moderately reduced activity, respectively, relative to the wild-type template (Fig. 7, *A* and *B*, *lanes 15* and *16*). Note that the stimulatory effect of the single AloopU mutation was no longer detected in the double mutants.

Taken together, these results strongly suggest an NC-dependent interaction between nt 143–149 in the RNA template and nt 40–46 in the 3′ anticodon stem and variable loop of the tRNA primer. This interaction modulates the efficiency of initiation of reverse transcription and replaces the requirement for additional downstream bases in templates smaller than RNA 224. Importantly, none of the mutations affected (−) SSDNA synthesis initiated by the R18 primer in the presence or absence of NC (data not shown), thus confirming that the effect is tRNA-specific.

DISCUSSION

In the present study, we have investigated the possible role of HIV-1 RNA template sequences immediately downstream of the PBS in the initiation of (−) SSDNA synthesis, using a reconstituted *in vitro* system. Our results demonstrate that in the absence of NC, at least 24 bases downstream of the PBS are required for maximal synthesis of (−) SSDNA with the $tRNA_3^{Lys}$ and R18 primers; in contrast, with the D18 primer, no additional bases beyond the PBS are needed. Interestingly, in the presence of NC, downstream bases are dispensable for tRNA-primed (−) SSDNA synthesis but are still required when the R18 primer is used.

The specific differences that we observe in the priming activities of RNA and DNA primers (Fig. 2) have not been reported previously but are consistent with kinetic (1–3, 5) and mutational (see below) (73, 74) studies of HIV-1 RT activity indicating that the efficiency of (−) SSDNA synthesis is sensitive to the helical conformation of primer-template complexes. The data are also consistent with structural studies of HIV-1 RT complexed to DNA or RNA primers annealed to a DNA template (15–17).

To further investigate the role of helical conformation in the initiation step, we assayed the priming activities of chimeric

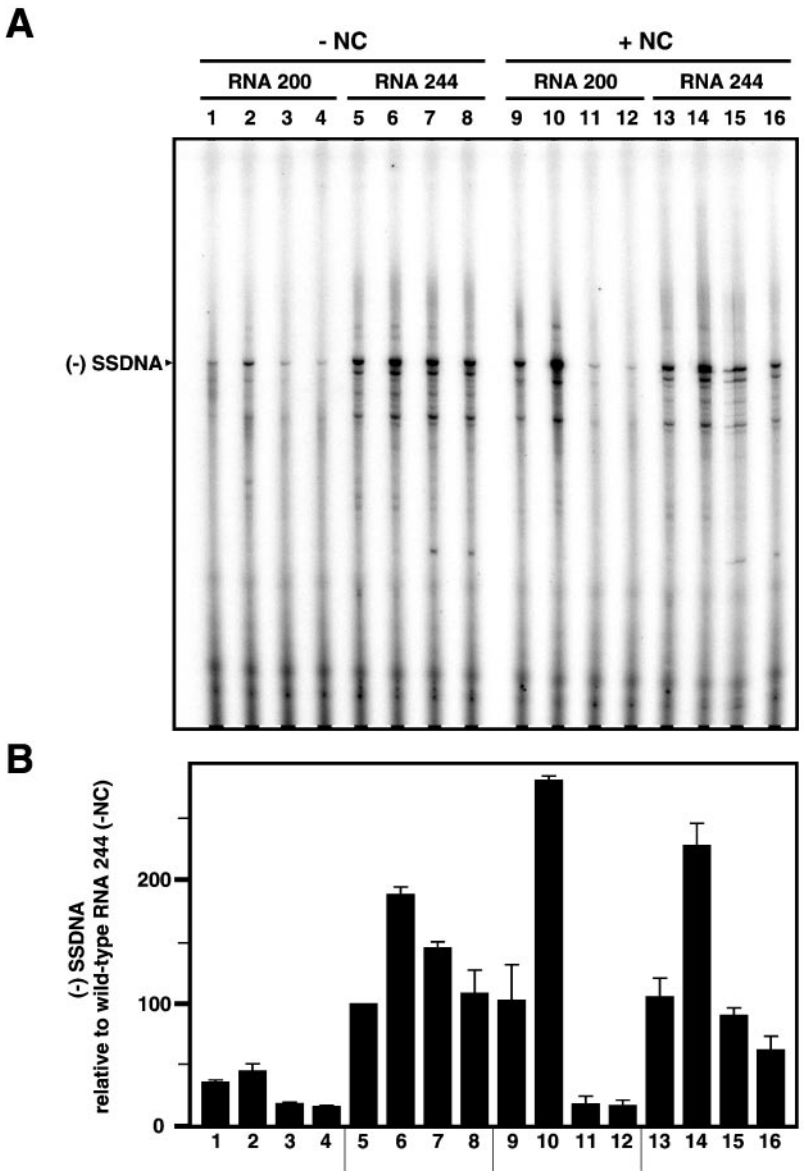

FIG. 7. **Effect of substitution mutations upstream of the PBS in templates RNA 200 and RNA 244 on (−) SSDNA synthesis primed by $tRNA_3^{Lys}$ in the absence or presence of NC.** *A*, gel data. (−) SSDNA synthesis was initiated with unlabeled native $tRNA_3^{Lys}$ primer in the absence (*lanes 1–8*) or presence of NC (*lanes 9–16*), as described under "Experimental Procedures." The DNA products synthesized with the RNA 200 and RNA 244 templates are shown in *lanes 1–4* and *lanes 9–12*, and *lanes 5–8* and *lanes 13–16*, respectively. The templates used were as follows: wild-type, *lanes 1* and *9* and *lanes 5* and *13*; AloopU, *lanes 2* and *10* and *lanes 6* and *14*; mut (143–149), *lanes 3* and *11* and *lanes 7* and *15*; and mut (143–149)/AloopU, *lanes 4* and *12* and *lanes 8* and *16*. The position of (−) SSDNA is indicated by an *arrow* to the *left* of the *gel*. *B*, PhosphorImager analysis of gel data averaged from three independent experiments. The data are expressed as (−) SSDNA relative to that made by the wild-type RNA 244 template in the absence of NC (100%). The *number below* each *bar* corresponds to the *lane numbers* in *A*.

DNA-RNA primers (Fig. 3). In addition, we also analyzed the CD spectra and thermostabilities of 18-nt primer:PBS duplexes (see Fig. 4 and Table I). As might be expected, the R18 duplex exhibits classical A-form geometry, whereas the D18 complex shows an intermediate (12–14, 75, 76) conformation (Fig. 4). Interestingly, the presence of a 3′ deoxyribonucleotide in the primer (R17D1) is not sufficient to alter RNA-like behavior in assays of (−) SSDNA synthesis (Fig. 3*C*) or duplex conformation relative to that of the all-RNA, R18 primer (data not shown). In contrast, the presence of nine deoxyribonucleotides at the 3′ end (R9D9), but not at the 5′ end (D9R9), of the primer has a dramatic effect on the requirement for additional template sequences and also affects duplex conformation. Thus, duplexes that maintain greater A-like character ((R18:PBS, D9R9:PBS) (Fig. 4*B*), and R17D1:PBS (data not shown)) show a stronger dependence on downstream template sequences (see Fig. 2*B* and Fig. 3, *B* and *C*, respectively), whereas a shift toward B-like conformation (D18:PBS and R9D9:PBS) (Fig. 4*A*) is correlated with a lack of a dependence on template length (see Fig. 2*A* and Fig. 3*A*, respectively). Melting studies of the 18-nt duplexes are in agreement with these data (Table I); R9D9 and D18 duplexes have similar T_m values, which are several degrees lower than the values obtained for the R18 and D9R9 duplexes.

Taken together, these results highlight the importance of both helical conformation and thermostability as determinants of priming activity in the initiation of minus-strand DNA synthesis. Interestingly, helical conformation also has a dramatic effect on the initiation of HIV-1 plus-strand DNA synthesis by the 15-nt RNA PPT primer. We demonstrated previously (73, 74) that plus-strand initiation is dependent on nucleic acid contacts with "primer grip" residues (16) in the palm subdomain of the p66 subunit of RT. Thus, aromatic substitution (73) and alanine-scanning mutations (74) in these residues abolish plus-strand priming activity with an RNA PPT primer but do not affect priming with a DNA version of the PPT. Gel shift experiments with RNA or DNA PPT primer-template complexes demonstrated that the efficiency of binding to RT is the same with an RNA or DNA PPT primer; therefore, differences in binding affinity could not account for the observed differences in priming activity (74). These results led to the conclusion that the unusual helical structure of the RNA PPT is a major determinant of plus-strand priming activity (74). In addition, these same primer grip mutations significantly reduce or in some cases completely block priming of minus-strand DNA synthesis by an R18 or a synthetic $tRNA_3^{Lys}$ primer while

having no effect on priming by a D18 primer (73, 74). By analogy to the PPT primers, the binding affinities of the RNA or D18 primer-template duplexes to RT might not have a major influence on priming in minus-strand synthesis, as well. Thus, we conclude that the correct structure of RT in the primer grip region, as well as the helical conformation of the primer, are critical for efficient initiation of both minus- and plus-strand DNA synthesis.

In the absence of NC, we have also demonstrated that for maximal synthesis of (−) SSDNA, at least 24 bases in the RNA template, immediately downstream of the PBS, are required if RNA primers are used (Fig. 2, *B* and *C*). These results are generally in accord with earlier *in vitro* data indicating that extension of $tRNA_3^{Lys}$ is less efficient if mutant RNA templates contain deletions of sequences within a 54-nt downstream region (4, 55, 56). However, the present findings and other data (46) appear to be at variance with the observation that the primer activation signal increases (−) SSDNA synthesis when downstream bases are mutated (53, 54).

How can we rationalize the requirement for additional downstream bases in the viral RNA template? The secondary structure of HIV-1 NL4-3 5′ genomic RNA depicted in Fig. 1*A* shows that sequences between nt 218 and 224 form a stem by base-pairing with the sequences from nt 126 to 132. This stem structure is highly conserved in HIV-1 (data not shown), and it seems possible that the additional 24 downstream bases might be important to maintain this stem structure and thereby stabilize the initiation complex when NC is not present. A more stable complex may also contribute to enhanced binding of the complex to RT.

To determine whether it is possible to predict formation of a more stable complex when the additional template bases are present, we performed *mfold* analysis (60, 61) on the U5 RNA sequence beginning at nt 113 and extending to nt 200–244 (Fig. 1); the 18-nt PBS was constrained by annealing to the 3′ 18 nt of $tRNA_3^{Lys}$. The analysis showed that RNA 200 has a ΔG value of −18.7 kcal/mol, whereas the ΔG values for RNA 224 and RNA 244 are −24.1 and −32.4 kcal/mol, respectively. These data are in agreement with the results shown in Fig. 2, *B* and *C* and support the idea that the longer templates assume conformations that favor annealing to R18 or $tRNA_3^{Lys}$, which, in turn, would result in formation of a more stable binary complex. Apparently, the contribution of nt 201–224 is sufficient for this effect, and therefore, RNA 224 is able to form the secondary structure required for efficient (−) SSDNA synthesis. This correlates well with the previous observation that an HIV-1 MAL RNA template consisting only of nt 123–217 has a very similar overall secondary structure as a longer HIV-1 MAL template consisting of nt 1–311 (11, 44, 46).

One of the most dramatic findings to emerge from this study concerns the ability of NC to abrogate the requirement for additional downstream bases in templates smaller than RNA 224 (Fig. 5). The NC effect was observed regardless of whether heat or NC annealing was used to form the binary complex (data not shown). The equivalence of heat and NC annealing has been shown by Brulé *et al.* (72), but this finding differs from reports by Rong *et al.* (38, 39), possibly because of different experimental conditions. It is of interest to note that when the dNTP concentrations are set at 5 μM (conditions that favor RT pausing), NC also has a significant stimulatory effect on (−) SSDNA synthesis with the RNA 224 and 244 templates (data not shown), probably because NC reduces pausing at secondary structure sites in viral RNA (57, 77). This observation raises the possibility that in the cell, where dNTPs are thought to be present at relatively low concentrations (78), NC may facilitate formation of the most stable template RNA conformation for efficient minus-strand DNA synthesis, even with genome-size viral RNA.

Because the NC effect is seen only with tRNA and not with R18 (Fig. 5), we speculated that NC nucleic acid chaperone activity may be stabilizing extended interactions between the tRNA primer and the RNA template. We considered the possibility that the interaction between residues in the A-rich loop and the anticodon loop of $tRNA_3^{Lys}$ promote efficient (−) SSDNA synthesis (1, 9). However, although it has been reported that substitution of the six residues in the A-rich loop (nt 162–167 in HIV-1 MAL; GUAAAA) with five residues (CUAUG) can significantly reduce (−) SSDNA synthesis *in vitro* (1), others have shown that deletion of the four A residues in HIV-1 HXB2 RNA leads to synthesis of slightly lower or very similar amounts of (−) SSDNA over time (4, 49, 79). Under the standard conditions used in our system (HIV-1 NL4-3), mutation of the four A residues to four U residues increases (−) SSDNA synthesis by ~1.5–3-fold, in agreement with the conclusion that removal of the four A residues eliminates pause sites that impede reverse transcription (data not shown) (4, 8, 49). The discrepancy between the results with different mutations and HIV-1 strains may reflect the different effects of each of these mutations on the conformation of the specific viral RNA-tRNA complex.

We also investigated whether an extended interaction between the 3′ arm of the anticodon stem and variable loop of $tRNA_3^{Lys}$ and nt 143–149 in the template is related to the NC effect. On the basis of modeling experiments, this interaction has been suggested to promote RT binding by preventing steric clashes between RT and the binary nucleic acid complex (11). In our experiments, we found that mutation of nt 143–149 alone or in combination with the AloopU mutation leads to a severe reduction in the activity of RNA 200 in reactions with NC (Fig. 7). The fact that the two mutants make the same absolute amount of (−) SSDNA in the absence or presence of NC suggests that even when NC is missing, this interaction plays some role in synthesis of (−) SSDNA, perhaps by affecting the conformation of the initiation complex. In contrast, under our usual assay conditions, RNA 244 template activity is the same in the presence or absence of NC (Fig. 7) and is not reduced by the single mutation in nt 143–149 (Fig. 7). The small reduction in the activity of the RNA 244 double mutant in the presence of NC may reflect partial destabilization of the initiation complex, which NC and/or the downstream sequences cannot overcome. Viewed in their entirety, these results provide strong evidence that the nucleic acid chaperone activity of NC modulates the stability of the initiation complex by favoring an interaction between the 3′ anticodon stem and variable loop of the tRNA and complementary sequences in the template. In the absence of NC, bases downstream of the PBS also contribute to stabilization of the initiation complex and promote efficient synthesis of (−) SSDNA. Experiments are currently in progress to further investigate the nature of the anticodon stem/variable loop-template interaction and the role of NC in this process.

In summary, we have shown that the differences in the activities of RNA, DNA, and chimeric DNA-RNA primers in the initiation of reverse transcription are related to differences in helical conformation and thermal stability of the primer-template complexes. When RNA primers are used in the absence of NC, the template must contain a minimum of 24 bases downstream of the PBS to achieve efficient (−) SSDNA synthesis, presumably because the additional bases lead to a more stable conformation of the viral RNA template. A similar requirement for downstream elements is observed with chimeric DNA-RNA primers that mimic the conformation and stability of the all-

RNA primer. NC abrogates this requirement only in the case of the full-length tRNA primer by stabilizing the interaction between the 3′ anticodon stem and variable loop of the tRNA and nt 143–149 in the RNA template. Taken together, these data support an important functional role for NC-facilitated tRNA-template interactions in initiation of reverse transcription *in vitro*.

Acknowledgments—We thank Dr. Besik I. Kankia for assistance with the CD analysis, as well as helpful discussion. We are also indebted to Dr. Robert Gorelick for the generous gift of the recombinant NC protein used in this work.

REFERENCES

1. Isel, C., Lanchy, J. M., Le Grice, S. F. J., Ehresmann, C., Ehresmann, B., and Marquet, R. (1996) *EMBO J.* **15,** 917–924
2. Lanchy, J. M., Ehresmann, C., Le Grice, S. F. J., Ehresmann, B., and Marquet, R. (1996) *EMBO J.* **15,** 7178–7187
3. Lanchy, J. M., Keith, G., Le Grice, S. F. J., Ehresmann, B., Ehresmann, C., and Marquet, R. (1998) *J. Biol. Chem.* **273,** 24425–24432
4. Liang, C., Rong, L., Götte, M., Li, X., Quan, Y., Kleiman, L., and Wainberg, M. A. (1998) *J. Biol. Chem.* **273,** 21309–21315
5. Thrall, S. H., Krebs, R., Wöhrl, B. M., Cellai, L., Goody, R. S., and Restle, T. (1998) *Biochemistry* **37,** 13349–13358
6. Beerens, N., and Berkhout, B. (2000) *J. Biol. Chem.* **275,** 15474–15481
7. Beerens, N., Groot, F., and Berkhout, B. (2000) *Nucleic Acids Res.* **28,** 4130–4137
8. Arts, E. J., Stetor, S. R., Li, X., Rausch, J. W., Howard, K. J., Ehresmann, B., North, T. W., Wöhrl, B. M., Goody, R. S., Wainberg, M. A., and Le Grice, S. F. J. (1996) *Proc. Natl. Acad. Sci. U. S. A.* **93,** 10063–10068
9. Isel, C., Marquet, R., Keith, G., Ehresmann, C., and Ehresmann, B. (1993) *J. Biol. Chem.* **268,** 25269–25272
10. Isel, C., Ehresmann, C., Keith, G., Ehresmann, B., and Marquet, R. (1995) *J. Mol. Biol.* **247,** 236–250
11. Isel, C., Westhof, E., Massire, C., Le Grice, S. F. J., Ehresmann, B., Ehresmann, C., and Marquet, R. (1999) *EMBO J.* **18,** 1038–1048
12. Arnott, S., Chandrasekaran, R., Millane, R. P., and Park, H. S. (1986) *J. Mol. Biol.* **188,** 631–640
13. Fedoroff, O. Y., Salazar, M., and Reid, B. R. (1993) *J. Mol. Biol.* **233,** 509–523
14. Szyperski, T., Götte, M., Billeter, M., Perola, E., Cellai, L., Heumann, H., and Wüthrich, K. (1999) *J. Biomol. NMR* **13,** 343–355
15. Ding, J., Das, K., Hsiou, Y., Sarafianos, S. G., Clark, A. D., Jr., Jacobo-Molina, A., Tantillo, C., Hughes, S. H., and Arnold, E. (1998) *J. Mol. Biol.* **284,** 1095–1111
16. Jacobo-Molina, A., Ding, J., Nanni, R. G., Clark, A. D., Jr., Lu, X., Tantillo, C., Williams, R. L., Kamer, G., Ferris, A. L., Clark, P., Hizi, A., Hughes, S. H., and Arnold, E. (1993) *Proc. Natl. Acad. Sci. U. S. A.* **90,** 6320–6324
17. Sarafianos, S. G., Das, K., Tantillo, C., Clark, A. D., Jr., Ding, J., Whitcomb, J. M., Boyer, P. L., Hughes, S. H., and Arnold, E. (2001) *EMBO J.* **20,** 1449–1461
18. Coffin, J. M., Hughes, S. H., and Varmus, H. E. (1997) *Retroviruses*, Cold Spring Harbor Laboratory Press, Cold Spring Harbor, NY
19. Cristofari, G., and Darlix, J. L. (2002) *Prog. Nucleic Acids Res. Mol. Biol.* **72,** 223–268
20. Darlix, J. L., Lapadat-Tapolsky, M., de Rocquigny, H., and Roques, B. P. (1995) *J. Mol. Biol.* **254,** 523–537
21. Herschlag, D. (1995) *J. Biol. Chem.* **270,** 20871–20874
22. Rein, A., Henderson, L. E., and Levin, J. G. (1998) *Trends Biochem. Sci.* **23,** 297–301
23. Tsuchihashi, Z., and Brown, P. O. (1994) *J. Virol.* **68,** 5863–5870
24. Williams, M. C., Rouzina, I., Wenner, J. R., Gorelick, R. J., Musier-Forsyth, K., and Bloomfield, V. A. (2001) *Proc. Natl. Acad. Sci. U. S. A.* **98,** 6121–6126
25. Williams, M. C., Gorelick, R. J., and Musier-Forsyth, K. (2002) *Proc. Natl. Acad. Sci. U. S. A.* **99,** 8614–8619
26. Guo, J., Wu, T., Kane, B. F., Johnson, D. G., Henderson, L. E., Gorelick, R. J., and Levin, J. G. (2002) *J. Virol.* **76,** 4370–4378
27. Guo, J., Wu, T., Anderson, J., Kane, B. F., Johnson, D. G., Gorelick, R. J., Henderson, L. E., and Levin, J. G. (2000) *J. Virol.* **74,** 8980–8988
28. Hong, M. K., Harbron, E. J., O'Connor, D. B., Guo, J., Barbara, P. F., Levin, J. G., and Musier-Forsyth, K. (2003) *J. Mol. Biol.* **325,** 1–10
29. Johnson, P. E., Turner, R. B., Wu, Z. R., Hairston, L., Guo, J., Levin, J. G., and Summers, M. F. (2000) *Biochemistry* **39,** 9084–9091
30. Khan, R., and Giedroc, D. P. (1992) *J. Biol. Chem.* **267,** 6689–6695
31. Cen, S., Huang, Y., Khorchid, A., Darlix, J. L., Wainberg, M. A., and Kleiman, L. (1999) *J. Virol.* **73,** 4485–4488
32. Feng, Y. X., Campbell, S., Harvin, D., Ehresmann, B., Ehresmann, C., and Rein, A. (1999) *J. Virol.* **73,** 4251–4256
33. Chan, B., Weidemaier, K., Yip, W. T., Barbara, P. F., and Musier-Forsyth, K. (1999) *Proc. Natl. Acad. Sci. U. S. A.* **96,** 459–464
34. De Rocquigny, H., Gabus, C., Vincent, A., Fournié-Zaluski, M. C., Roques, B., and Darlix, J. L. (1992) *Proc. Natl. Acad. Sci. U. S. A.* **89,** 6472–6476
35. Hargittai, M. R. S., Mangla, A. T., Gorelick, R. J., and Musier-Forsyth, K. (2001) *J. Mol. Biol.* **312,** 985–997
36. Lapadat-Tapolsky, M., Pernelle, C., Borie, C., and Darlix, J. L. (1995) *Nucleic Acids Res.* **23,** 2434–2441
37. Prats, A. C., Housset, V., de Billy, G., Cornille, F., Prats, H., Roques, B., and Darlix, J. L. (1991) *Nucleic Acids Res.* **19,** 3533–3541
38. Rong, L., Liang, C., Hsu, M., Guo, X., Roques, B. P., and Wainberg, M. A. (2001) *J. Biol. Chem.* **276,** 47725–47732
39. Rong, L., Liang, C., Hsu, M., Kleiman, L., Petitjean, P., de Rocquigny, H., Roques, B. P., and Wainberg, M. A. (1998) *J. Virol.* **72,** 9353–9358
40. Aiyar, A., Cobrinik, D., Ge, Z., Kung, H. J., and Leis, J. (1992) *J. Virol.* **66,** 2464–2472
41. Leis, J., Aiyar, A., and Cobrinik, D. (1993) in *Reverse Transcriptase* (Skalka, A. M., and Goff, S. P., eds) pp. 33–47, Cold Spring Harbor Laboratory Press, Cold Spring Harbor, NY
42. Morris, S., Johnson, M., Stavnezer, E., and Leis, J. (2002) *J. Virol.* **76,** 7571–7577
43. Miller, J. T., Ehresmann, B., Hübscher, U., and Le Grice, S. F. J. (2001) *J. Biol. Chem.* **276,** 27721–27730
44. Isel, C., Keith, G., Ehresmann, B., Ehresmann, C., and Marquet, R. (1998) *Nucleic Acids Res.* **26,** 1198–1204
45. Lanchy, J. M., Isel, C., Keith, G., Le Grice, S. F. J., Ehresmann, C., Ehresmann, B., and Marquet, R. (2000) *J. Biol. Chem.* **275,** 12306–12312
46. Goldschmidt, V., Rigourd, M., Ehresmann, C., Le Grice, S. F. J., Ehresmann, B., and Marquet, R. (2002) *J. Biol. Chem.* **277,** 43233–43242
47. Huang, Y., Shalom, A., Li, Z., Wang, J., Mak, J., Wainberg, M. A., and Kleiman, L. (1996) *J. Virol.* **70,** 4700–4706
48. Kang, S. M., Zhang, Z., and Morrow, C. D. (1997) *J. Virol.* **71,** 207–217
49. Liang, C., Li, X., Rong, L., Inouye, P., Quan, Y., Kleiman, L., and Wainberg, M. A. (1997) *J. Virol.* **71,** 5750–5757
50. Puglisi, E. V., and Puglisi, J. D. (1998) *Nat. Struct. Biol.* **5,** 1033–1036
51. Skripkin, E., Isel, C., Marquet, R., Ehresmann, B., and Ehresmann, C. (1996) *Nucleic Acids Res.* **24,** 509–514
52. Wakefield, J. K., Kang, S. M., and Morrow, C. D. (1996) *J. Virol.* **70,** 966–975
53. Beerens, N., and Berkhout, B. (2002) *J. Virol.* **76,** 2329–2339
54. Beerens, N., Groot, F., and Berkhout, B. (2001) *J. Biol. Chem.* **276,** 31247–31256
55. Li, X., Liang, C., Quan, Y., Chandok, R., Laughrea, M., Parniak, M. A., Kleiman, L., and Wainberg, M. A. (1997) *J. Virol.* **71,** 6003–6010
56. Liang, C., Rong, L., Russell, R. S., and Wainberg, M. A. (2000) *J. Virol.* **74,** 6251–6261
57. Wu, W., Henderson, L. E., Copeland, T. D., Gorelick, R. J., Bosche, W. J., Rein, A., and Levin, J. G. (1996) *J. Virol.* **70,** 7132–7142
58. Adachi, A., Gendelman, H. E., Koenig, S., Folks, T., Willey, R., Rabson, A., and Martin, M. A. (1986) *J. Virol.* **59,** 284–291
59. Guo, J., Henderson, L. E., Bess, J., Kane, B., and Levin, J. G. (1997) *J. Virol.* **71,** 5178–5188
60. Zuker, M., Mathews, D. H., and Turner, D. H. (1999) in *RNA Biochemistry and Biotechnology* (Barciszewski, J., and Clark, B. F. C., eds) pp. 11–43, Kluwer Academic Publishers, Dordrecht, The Netherlands
61. Mathews, D. H., Sabina, J., Zuker, M., and Turner, D. H. (1999) *J. Mol. Biol.* **288,** 911–940
62. Guo, J., Wu, W., Yuan, Z. Y., Post, K., Crouch, R. J., and Levin, J. G. (1995) *Biochemistry* **34,** 5018–5029
63. Scaringe, S. A., Francklyn, C., and Usman, N. (1990) *Nucleic Acids Res.* **18,** 5433–5441
64. Sproat, B., Colonna, F., Mullah, B., Tsou, D., Andrus, A., Hampel, A., and Vinayak, R. (1995) *Nucleosides Nucleotides* **14,** 255–273
65. Gyi, J. I., Conn, G. L., Lane, A. N., and Brown, T. (1996) *Biochemistry* **35,** 12538–12548
66. Kankia, B. I., and Marky, L. A. (1999) *J. Phys. Chem. B* **103,** 8759–8767
67. Sugimoto, N., Nakano, S., Katoh, M., Matsumura, A., Nakamuta, H., Ohmichi, T., Yoneyama, M., and Sasaki, M. (1995) *Biochemistry* **34,** 11211–11216
68. Wahl, M. C., and Sundaralingam, M. (2000) *Nucleic Acids Res.* **28,** 4356–4363
69. Yang, J. T., and Samejima, T. (1969) *Prog. Nucleic Acids Res. Mol. Biol.* **9,** 223–300
70. Lesnik, E. A., and Freier, S. M. (1995) *Biochemistry* **34,** 10807–10815
71. Ratmeyer, L., Vinayak, R., Zhong, Y. Y., Zon, G., and Wilson, W. D. (1994) *Biochemistry* **33,** 5298–5304
72. Brulé, F., Marquet, R., Rong, L., Wainberg, M. A., Roques, B. P., Le Grice, S. F. J., Ehresmann, B., and Ehresmann, C. (2002) *RNA* **8,** 8–15
73. Ghosh, M., Williams, J., Powell, M. D., Levin, J. G., and Le Grice, S. F. J. (1997) *Biochemistry* **36,** 5758–5768
74. Powell, M. D., Ghosh, M., Jacques, P. S., Howard, K. J., Le Grice, S. F. J., and Levin, J. G. (1997) *J. Biol. Chem.* **272,** 13262–13269
75. Horton, N. C., and Finzel, B. C. (1996) *J. Mol. Biol.* **264,** 521–533
76. Salazar, M., Fedoroff, O. Y., Miller, J. M., Ribeiro, N. S., and Reid, B. R. (1993) *Biochemistry* **32,** 4207–4215
77. Ji, X., Klarmann, G. J., and Preston, B. D. (1996) *Biochemistry* **35,** 132–143
78. Roy, B., Beuneu, C., Roux, P., Buc, H., Lemaire, G., and Lepoivre, M. (1999) *Anal. Biochem.* **269,** 403–409
79. Li, X., Quan, Y., Arts, E. J., Li, Z., Preston, B. D., de Rocquigny, H., Roques, B. P., Darlix, J. L., Kleiman, L., Parniak, M. A., and Wainberg, M. A. (1996) *J. Virol.* **70,** 4996–5004

Efficient Initiation of HIV-1 Reverse Transcription*in Vitro* : REQUIREMENT FOR RNA SEQUENCES DOWNSTREAM OF THE PRIMER BINDING SITE ABROGATED BY NUCLEOCAPSID PROTEIN-DEPENDENT PRIMER-TEMPLATE INTERACTIONS

Yasumasa Iwatani, Abbey E. Rosen, Jianhui Guo, Karin Musier-Forsyth and Judith G. Levin

J. Biol. Chem. 2003, 278:14185-14195.
doi: 10.1074/jbc.M211618200 originally published online January 30, 2003
